

# On Uniform Semiglobal Exponential Stability (USGES) of Proportional Line-of-Sight Guidance Laws

Thor I. Fossen<sup>a</sup> and Kristin Y. Pettersen<sup>a</sup>

<sup>a</sup>Centre for Autonomous Marine Operations and Systems (AMOS), Department of Engineering Cybernetics, Norwegian University of Science and Technology, 7491 Trondheim, Norway

---

## Abstract

This paper presents a uniform semiglobal exponential stability (USGES) proof for a class of proportional line-of-sight (LOS) guidance laws used for vehicle path-following control. The LOS guidance law under consideration is a lookahead-based guidance law for marine craft. The USGES proof extends previous results that only guarantee global  $\kappa$ -exponential stability. Typical applications are marine craft and aircraft motion control systems for path following where the total system is a cascade of the motion controller and guidance law error dynamics.

*Key words:* Guidance systems; marine systems; autonomous vehicles; kinematics.

---

## 1 Introduction

Surface vehicles, aircraft and marine craft use proportional guidance laws to accomplish desired motion control scenario such as object tracking, path following, path tracking and path maneuvering; see Breivik and Fossen (2009), Fossen (2011), Lekkas and Fossen (2013), and Yanushevsky (2011) for instance. For three degrees-of-freedom (DOF) path-following applications, the control objective is to follow a predefined planar path without needing to set time constraints. A popular and effective way to achieve convergence to the desired path is to implement a lookahead-based LOS guidance law mimicking an experienced sailor. This method exploits the geometry of the problem and generates a reference trajectory for the desired course or heading angle, which is used by the autopilot.

Guided LOS motion control of AUVs using sliding mode control for stabilizing the combined speed, steering and diving responses was addressed by Healey and Lienard (1993). In this work, the stability properties of the proportional LOS guidance law were not analyzed. Uniform global asymptotic stability (UGAS) and uniform local exponential stability (ULES) of the proportional LOS

guidance law was first proven by Pettersen and Lefeber (2001) in connection with a simplified vehicle model. UGAS/ULES is also referred to as *global  $\kappa$ -exponential stability* as defined by Sørдалen and Egeland (1995). The result of Pettersen and Lefeber (2001) was further extended to include a more complete vehicle model by Børhaug and Pettersen (2005), and Fredriksen and Pettersen (2006).

The main contribution of the paper is prove that the equilibrium point of the Healey and Lienard (1993) proportional LOS guidance law is USGES as opposed to previous results that only prove global  $\kappa$ -exponential stability. USGES is slightly weaker than global exponential stability (GES) but GES cannot be achieved for this type of system due to the kinematic representation, which introduces saturation through the trigonometric functions. The LOS guidance law is very popular since it mimics an experienced sailor and it is important to establish proper stability properties for state-of-the-art guidance laws. Furthermore, the USGES stability property is important for systems that are exposed to environmental disturbances, in particular to quantify robustness. Finally, we show that the USGES property also can be proven for a ship model in cascade with the LOS guidance law.

### 1.1 Cross-track error

Let  $\theta \geq 0$  denote the path variable. A formula for the cross-track error can be derived by considering a two-

---

\* This paper was not presented at any IFAC meeting. Corresponding author T. I. Fossen. Tel. +47-91897361. Fax. +4773594599

*Email addresses:* Thor.Fossen@ntnu.no (Thor I. Fossen), Kristin.Y.Pettersen@itk.ntnu.no (Kristin Y. Pettersen).

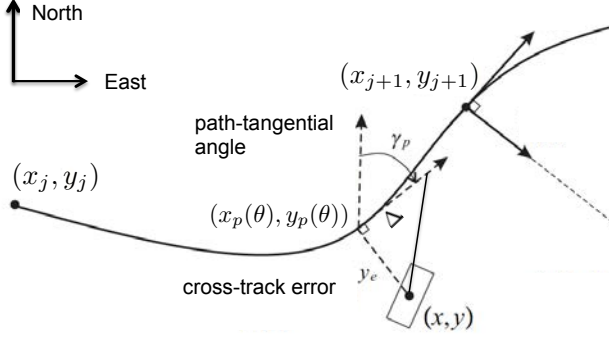


Fig. 1. LOS guidance geometry. The desired course angle  $\chi$  given by (16) is determined such that the vehicle velocity is directed towards a point that is located a user specified distance  $\Delta$  (lookahead distance) on the path tangent.  $\gamma_p$  is the path-tangential angle and  $y_e$  is the cross-track error.

dimensional (2-D)  $\mathcal{C}^1$  parametrized path  $(x_p(\theta), y_p(\theta))$  which is assumed to go through a set of successive waypoints  $(x_j, y_j)$  for  $j = 1, 2, \dots, N$  as illustrated in Figure 1. For any point  $(x_p(\theta), y_p(\theta))$  along the path, the path-tangential reference frame is rotated an angle:

$$\gamma_p(\theta) = \text{atan2}(y'_p(\theta), x'_p(\theta)) \quad (1)$$

with respect to the North-East reference frame. Note that for a straight line  $\gamma_p = \text{atan2}(y_{j+1} - y_j, x_{j+1} - x_j)$  is constant between the waypoints. For a vehicle located at the position  $(x, y)$  the cross-track error is computed as the orthogonal distance to the path-tangential reference frame defined by the point  $(x_p(\theta), y_p(\theta))$ . Hence,

$$\begin{bmatrix} 0 \\ y_e \end{bmatrix} = \underbrace{\begin{bmatrix} \cos(\gamma_p(\theta)) & \sin(\gamma_p(\theta)) \\ -\sin(\gamma_p(\theta)) & \cos(\gamma_p(\theta)) \end{bmatrix}^\top}_{\mathbf{R}^\top(\gamma_p(\theta))} \begin{bmatrix} x - x_p(\theta) \\ y - y_p(\theta) \end{bmatrix} \quad (2)$$

where  $\mathbf{R}(\gamma_p(\theta)) \in SO(2)$ . Expanding (2) gives the normal line:

$$y - y_p(\theta) = -\frac{1}{\tan(\gamma_p(\theta))}(x - x_p(\theta)) \quad (3)$$

through  $(x_p(\theta), y_p(\theta))$  and the cross-track error:

$$y_e = -(x - x_p(\theta)) \sin(\gamma_p(\theta)) + (y - y_p(\theta)) \cos(\gamma_p(\theta)) \quad (4)$$

where  $\theta$  propagates according to (Fossen, 2011):

$$\dot{\theta} = \frac{U}{\sqrt{x'_p(\theta)^2 + y'_p(\theta)^2}} > 0 \quad (5)$$

As pointed out by Samson (1992) there may be infinite solutions of (3) if the path is a closed curve. In the following we will assume that the path is an open curve,

i.e. the end point is different from the start point. Definition 1 guarantees that there is a unique solution for the cross-track error  $y_e$  obtained by minimizing  $\theta$ .

**Definition 1 (Uniqueness of solutions)** *The unique solution of (4) is denoted  $y_e(\theta^*)$  and is defined by:*

$$\theta^* := \arg \min_{\theta \geq 0} \left\{ \frac{U^2}{x'_p(\theta)^2 + y'_p(\theta)^2} \right\} \quad (6)$$

subject to

$$y - y_p(\theta) = -\frac{1}{\tan(\gamma_p(\theta))}(x - x_p(\theta)) \quad (7)$$

This is a nonlinear optimization problem, which can be solved numerically. However, for many paths  $\theta^*$  can be found by computing all possible projection candidates  $\theta_i$  ( $i = 1, \dots, M$ ) given by (3) and choose the one closest to the previous  $\theta^*$ -value.

## 1.2 Kinematic equations

The kinematic equations can be expressed in terms of the surge, sway and yaw velocities  $u, v$  and  $r$ , respectively. In Fossen (2011, Chapter 2) it was shown that:

$$\dot{x} = u \cos(\psi) - v \sin(\psi) \quad (8)$$

$$\dot{y} = u \sin(\psi) + v \cos(\psi) \quad (9)$$

$$\dot{\psi} = r \quad (10)$$

where  $\psi$  is the yaw angle. Differentiation of (4) gives:

$$\dot{y}_e = -(\dot{x} - \dot{x}_p(\theta)) \sin(\gamma_p) + (\dot{y} - \dot{y}_p(\theta)) \cos(\gamma_p) - [(x - x_p(\theta)) \cos(\gamma_p) + (y - y_p(\theta)) \sin(\gamma_p)] \dot{\gamma}_p \quad (11)$$

The last line in (11) is zero because of (3). From (1) it follows that  $\dot{x}_p(\theta) \sin(\gamma_p(\theta)) - \dot{y}_p(\theta) \cos(\gamma_p(\theta)) = 0$ . Consequently, (8), (9) and (11) give:

$$\begin{aligned} \dot{y}_e &= -\dot{x} \sin(\gamma_p(\theta)) + \dot{y} \cos(\gamma_p(\theta)) \\ &= -(u \cos(\psi) - v \sin(\psi)) \sin(\gamma_p(\theta)) \\ &\quad + (u \sin(\psi) + v \cos(\psi)) \cos(\gamma_p(\theta)) \end{aligned} \quad (12)$$

This can be written in *amplitude-phase form*:

$$\dot{y}_e = U \sin(\psi - \gamma_p(\theta) + \beta) \quad (13)$$

where the amplitude  $U = \sqrt{u^2 + v^2}$  and phase  $\beta = \text{atan2}(v, u)$  are recognized as the *speed* and *sideslip angle*, respectively. A vehicle exposed to drift forces (wind, waves and ocean currents) exhibits variations in the velocities  $u, v$  and  $r$  according to *Newton's second law*, which defines the *kinetic* equations of motion. The response can be observed as a non-zero sideslip angle  $\beta$

during path following. This is also observed as a difference in heading angle  $\psi$  and course angle  $\chi$  according to:

$$\chi = \psi + \beta \quad (14)$$

This implies that (13) can be written:

$$\dot{y}_e = U \sin(\chi - \gamma_p(\theta)) \quad (15)$$

## 2 LOS proportional guidance law

Equation (13) is similar to the formulae used by Healey and Lienard (1993), Pettersen and Lefeber (2001), Børhaug and Pettersen (2005), Breivik and Fossen (2005), Fredriksen and Pettersen (2006), and Breivik and Fossen (2009). The proportional LOS guidance law for (15) is chosen as:

$$\chi = \gamma_p(\theta) + \tan^{-1} \left( -\frac{y_e}{\Delta} \right) \quad (16)$$

where  $0 < \Delta_{\min} \leq \Delta \leq \Delta_{\max}$ . Hence, by inserting (16) into (15) and using,  $\sin(\tan^{-1}(x)) = x/\sqrt{1+x^2}$ , gives:

$$\dot{y}_e = -\frac{U}{\sqrt{\Delta^2 + y_e^2}} y_e \quad (17)$$

Notice that cross-track error dynamics (17) is nonautonomous since both  $U$  and  $\Delta$  can be time-varying. The look-ahead distance can be made time-dependent using optimization techniques (Pavlov et al., 2009) or explicit formulae (Lekkas and Fossen, 2012).

### Theorem 1 (Proportional LOS guidance law)

The LOS guidance law (16) applied to the cross-track error dynamics (15) renders the equilibrium point  $\dot{y}_e = 0$  USGES if the look-ahead distance and speed satisfy  $0 < \Delta_{\min} \leq \Delta \leq \Delta_{\max}$  and  $0 < U_{\min} \leq U \leq U_{\max}$ , respectively.

**PROOF.** See Appendix A.

**Remark 1** In addition to the convergence properties proven here being slightly stronger than the global  $\kappa$ -exponential stability proven in Fredriksen and Pettersen (2006), USGES is important from a robustness perspective. In particular, it is seen from Lemmas 9.2-3 in Khalil (2002) that ULAS and ULES both provide robustness to small uniformly bounded (UB) disturbances. It is, however, only the case of exponential stability that allows us to conclude anything about the robustness to larger uniformly bounded disturbances. It follows from Lemma 9.2 in Khalil (2002) that the USGES property implies that we always can choose a region of attraction in which we have exponential convergence sufficiently large. Hence,

we can always satisfy the condition for which the solution of the perturbed system will be UB irrespective of the size of the perturbation. USGES thus provides stronger robustness properties than global  $\kappa$ -exponential stability.

**Remark 2** Notice that GES cannot be achieved due to the structural properties of the cross-track error dynamics (15), which contains a sinusoidal function introducing saturation. As a consequence, the system gain in (17) decreases with the magnitude of the cross-track error and thus global exponential convergence cannot be achieved.

## 3 Application to ships: cascaded analysis

In this section we extend the results of Theorem 1 to include the ship dynamics. A similar approach can be taken for UAV and AUV guidance systems.

### 3.1 Ship dynamics

Consider the ship maneuvering model (Fossen, 2011):

$$\mathbf{M}\dot{\boldsymbol{\nu}} + \mathbf{C}(\boldsymbol{\nu})\boldsymbol{\nu} + \mathbf{D}\boldsymbol{\nu} = \boldsymbol{\tau} \quad (18)$$

where  $\boldsymbol{\nu} = [u, v, r]^T$  denotes the surge, sway and yaw velocities. The control inputs are:

$$\boldsymbol{\tau} = [\tau_u, Y_\delta\delta, N_\delta\delta]^T \quad (19)$$

where  $\tau_u$  is the control force in surge and  $\delta$  is the rudder angle. The rudder force  $Y_\delta\delta$  and moment  $N_\delta\delta$  affect the sway and yaw modes, respectively through the hydrodynamic derivatives  $Y_\delta$  and  $N_\delta$ . The system matrices in (18) can be expressed as:

$$\mathbf{M} = \begin{bmatrix} m_{11} & 0 & 0 \\ 0 & m_{22} & m_{23} \\ 0 & m_{23} & m_{33} \end{bmatrix} \quad \mathbf{D} = \begin{bmatrix} d_{11} & 0 & 0 \\ 0 & d_{22} & d_{23} \\ 0 & d_{32} & d_{33} \end{bmatrix} \quad (20)$$

$$\mathbf{C}(\boldsymbol{\nu}) = \begin{bmatrix} 0 & 0 & -m_{22}v - m_{23}r \\ 0 & 0 & m_{11}u \\ m_{22}v + m_{23}r & -m_{11}u & 0 \end{bmatrix} \quad (21)$$

where  $\mathbf{M}$ ,  $\mathbf{C}(\boldsymbol{\nu})$  and  $\mathbf{D}$  are the inertia, Coriolis/centripetal and damping matrices, respectively.

The rudder angle  $\delta$  is used to control the yaw dynamics similar to a heading autopilot while  $\tau_u$  is used for speed control. In order to deal with underactuation, it is convenient to express the equations of motion such that sway is not influenced by the rudder angle  $\delta$ . This can be achieved by moving the position measurement of the

ship to the *pivot point*  $(\bar{x}, \bar{y})$ , which is defined according to Tzeng (1998). Moreover,

$$\bar{x} := x + \varepsilon \cos(\psi) \quad (22)$$

$$\bar{y} := y + \varepsilon \sin(\psi) \quad (23)$$

$$\bar{v} := v + \varepsilon r \quad (24)$$

where  $\varepsilon = -(m_{33}Y_\delta - m_{23}N_\delta)/(m_{22}N_\delta - m_{23}Y_\delta)$ . This corresponds to moving the position along the body-fixed  $x$ -axis (the centerline) of the ship to the point where the rudder gives only a yaw moment and no sway force. Hence, the input  $\delta$  in the  $\bar{v}$ -dynamics is removed and

$$\dot{\bar{y}} = \sin(\psi)(\bar{u} + u_d) + \cos(\psi)\bar{v} \quad (25)$$

$$\dot{\psi} = r \quad (26)$$

$$\begin{aligned} \dot{\bar{v}} &= \dot{v} + \varepsilon \dot{r} \\ &= (\Upsilon \bar{u} + \Upsilon u_d + M)r + (\Lambda \bar{u} + \Lambda u_d + N)\bar{v} \end{aligned} \quad (27)$$

$$\dot{r} = \frac{\delta}{\Gamma} (m_{22}N_\delta - m_{23}Y_\delta) + \Omega r + F \bar{v} \quad (28)$$

$$\dot{\bar{u}} = \frac{1}{m_{11}} (\tau_u + (m_{22}v + m_{23}r)r - d_{11}u) \quad (29)$$

where  $\bar{u} = u - u_d$ ,  $u_d = \text{constant}$  is the desired surge velocity and

$$\begin{aligned} \Upsilon &= \frac{1}{\Gamma} (-2m_{23}m_{22}\varepsilon + m_{22}^2\varepsilon^2 + m_{23}^2 \\ &\quad - m_{22}m_{11}\varepsilon^2 - m_{33}m_{11} + 2m_{23}m_{11}\varepsilon) \end{aligned}$$

$$\begin{aligned} M &= \frac{1}{\Gamma} (m_{23}d_{33} - \varepsilon m_{22}d_{33} - m_{33}d_{23} - m_{23}d_{32}\varepsilon \\ &\quad + \varepsilon m_{23}d_{23} + m_{22}d_{32}\varepsilon^2 + m_{33}d_{22}\varepsilon - m_{23}d_{22}\varepsilon^2) \end{aligned}$$

$$\Lambda = \frac{1}{\Gamma} (m_{22}m_{11}\varepsilon - m_{22}^2\varepsilon - m_{23}m_{11} + m_{22}m_{23})$$

$$N = \frac{1}{\Gamma} (m_{23}d_{22}\varepsilon - m_{22}d_{32}\varepsilon - m_{33}d_{22} + m_{23}d_{32})$$

$$\begin{aligned} \Omega &= \frac{1}{\Gamma} (m_{23}m_{11}(\bar{u} + u_d) + m_{22}^2(\bar{u} + u_d)\varepsilon \\ &\quad - m_{23}d_{22}\varepsilon + m_{23}d_{23} - m_{22}m_{11}(\bar{u} + u_d)\varepsilon \\ &\quad - m_{22}(\bar{u} + u_d)m_{23} - m_{22}d_{33} + m_{22}d_{32}\varepsilon) \end{aligned}$$

$$\begin{aligned} F &= \frac{1}{\Gamma} (m_{23}d_{22} - m_{22}^2(\bar{u} + u_d) \\ &\quad - m_{22}d_{32} + m_{22}m_{11}(\bar{u} + u_d)) \end{aligned}$$

The cross-track error  $\bar{y}_e$  is defined as:

$$\bar{y}_e := -(\bar{x} - x_p(\theta)) \sin(\gamma_p(\theta)) + (\bar{y} - y_p(\theta)) \cos(\gamma_p(\theta)) \quad (30)$$

**Remark 3** *The cross-track error definition (30) means that the ship pivot point follows the path. This is indeed a very natural way of steering a ship, and it is what a practiced helmsman typically will do.*

Hence, (27) and (30) define the sway dynamics in the

pivot point:

$$\dot{\bar{y}}_e = \bar{U} \sin(\psi - \gamma_p(\theta) + \bar{\beta}) = \bar{U} \sin(\chi - \gamma_p(\theta)) \quad (31)$$

$$\dot{\bar{v}} = (\Upsilon \bar{u} + \Upsilon u_d + M)r + (\Lambda \bar{u} + \Lambda u_d + N)\bar{v} \quad (32)$$

where  $\chi = \psi + \bar{\beta}$ ,  $\bar{U} = \sqrt{(\bar{u} + u_d)^2 + \bar{v}^2}$  and  $\bar{\beta} = \text{atan2}(\bar{v}, \bar{u} + u_d)$ . The proportional LOS guidance law takes the form:

$$\chi_d = \gamma_p(\theta) + \tan^{-1} \left( -\frac{\bar{y}_e}{\Delta} \right) \quad (33)$$

### 3.2 Straight-line paths

We consider the special case where  $\gamma_p(\theta) = \gamma_p$  is constant and  $\bar{\beta} = 0$ , that is straight-line paths such that:

$$\dot{\bar{y}}_e = (\bar{u} + u_d) \sin(\psi - \gamma_p) + \bar{v} \cos(\psi - \gamma_p) = \bar{U} \sin(\psi - \gamma_p) \quad (34)$$

Due to the underactuation we have a dynamic system with both *external* and *internal* dynamics. The external dynamics consists of the surge and yaw equations (26), (28) and (29), which we can control directly using the control inputs  $\tau_u$  (surge force) and  $\delta$  (rudder angle). Furthermore, we have the underactuated dynamics, i.e. the sway dynamics (27) and (34), with states being the cross track error  $\bar{y}_e$  and the sway velocity  $\bar{v}$  for which we have no independent control inputs. This is the internal dynamics, and the stability of this dynamics needs to be analyzed carefully. It is well-known that the stability of the internal dynamics depends on the reference trajectories of the external dynamics (Isidori, 1989). We will in this section show that when the reference trajectory of the external state  $\psi$  is chosen to depend on the internal state  $\bar{y}_e$  in a way that is motivated by the experience of practiced helmsmen, i.e. using the proportional LOS guidance law (33), then the internal dynamics is USGES under certain conditions on the look-ahead-distance  $\Delta$ .

The course angle error dynamics is defined as  $z_1 := \chi - \chi_d = \psi - \gamma_p - \tan^{-1}(-\bar{y}_e/\Delta)$  and  $z_2 := \dot{z}_1$  and this together with the surge velocity (29) represent the external dynamics of the system. Using (26) and (28) the time derivatives of  $z_1$  and  $z_2$  become:

$$\dot{z}_1 = r + \frac{\dot{\bar{y}}_e \Delta}{\Delta^2 + \bar{y}_e^2} \quad (35)$$

$$\begin{aligned} \dot{z}_2 &= \frac{\delta}{\Gamma} (m_{22}N_\delta - m_{23}Y_\delta) + \Omega r + F \bar{v} \\ &\quad + \left( \frac{\Delta \ddot{\bar{y}}_e}{\Delta^2 + \bar{y}_e^2} - \frac{2\Delta \bar{y}_e (\dot{\bar{y}}_e)^2}{(\Delta^2 + \bar{y}_e^2)^2} \right) \end{aligned} \quad (36)$$

The control inputs  $\tau_u$  in surge and  $\delta$  in yaw are used to control the external system (29) and (35)–(36). Choos-

ing:

$$\begin{aligned}\tau_u &= -(m_{22}v + m_{23}r)r + d_{11}u + m_{11}(\dot{u}_d - k_u\bar{u}) \quad (37) \\ \delta &= \frac{\Gamma}{m_{22}N_\delta - m_{23}Y_\delta}(-\Omega r - F\bar{v} + \frac{2\Delta\bar{y}_e(\dot{\bar{y}}_e)^2}{(\Delta^2 + \bar{y}_e^2)^2} \\ &\quad - \frac{\Delta\ddot{\bar{y}}_e}{\Delta^2 + \bar{y}_e^2} - k_1z_2 - k_0z_1) \quad (38)\end{aligned}$$

where  $k_1 > 0, k_2 > 0$  and  $k_u > 0$  gives the closed-loop system:

$$\begin{aligned}\dot{\bar{y}}_e &= \frac{\sin(z_1)(\Delta(\bar{u} + u_d) + \bar{y}_e\bar{v})}{\sqrt{\Delta^2 + \bar{y}_e^2}} \\ &\quad + \frac{\cos(z_1)(\Delta\bar{v} - (\bar{u} + u_d)\bar{y}_e)}{\sqrt{\Delta^2 + \bar{y}_e^2}} \quad (39)\end{aligned}$$

$$\begin{aligned}\dot{\bar{v}} &= (\Lambda\bar{u} + \Lambda u_d + N)\bar{v} + \\ &\quad (\Upsilon\bar{u} + \Upsilon u_d + M)\left(z_2 - \frac{\dot{\bar{y}}_e\Delta}{\Delta^2 + \bar{y}_e^2}\right) \quad (40)\end{aligned}$$

$$\dot{z}_1 = z_2 \quad (41)$$

$$\dot{z}_2 = -k_1z_2 - k_0z_1 \quad (42)$$

$$\dot{\bar{u}} = -k_u\bar{u} \quad (43)$$

The error dynamics is a cascaded system:

$$\begin{aligned}\begin{bmatrix} \dot{\bar{y}}_e \\ \dot{\bar{v}} \end{bmatrix} &= \begin{bmatrix} -\frac{u_d}{\sqrt{\Delta^2 + \bar{y}_e^2}} & \frac{\Delta}{\sqrt{\Delta^2 + \bar{y}_e^2}} \\ X\frac{\Delta u_d}{(\sqrt{\Delta^2 + \bar{y}_e^2})^3} & Y - X\frac{\Delta^2}{(\sqrt{\Delta^2 + \bar{y}_e^2})^3} \end{bmatrix} \begin{bmatrix} \bar{y}_e \\ \bar{v} \end{bmatrix} \\ &\quad + \begin{bmatrix} h_{11} & 0 & h_{13} \\ h_{21} & h_{22} & h_{23} \end{bmatrix} \begin{bmatrix} z_1 \\ z_2 \\ \bar{u} \end{bmatrix} \quad (44)\end{aligned}$$

$$\begin{aligned}\begin{bmatrix} \dot{z}_1 \\ \dot{z}_2 \\ \dot{\bar{u}} \end{bmatrix} &= \begin{bmatrix} 0 & 1 & 0 \\ -k_0 & -k_1 & 0 \\ 0 & 0 & -k_u \end{bmatrix} \begin{bmatrix} z_1 \\ z_2 \\ \bar{u} \end{bmatrix} \quad (45)\end{aligned}$$

where  $X = \Upsilon u_d + M, Y = \Lambda u_d + N$  and

$$\begin{aligned}h_{11} &= \frac{\sin(z_1)}{z_1} \frac{\Delta(\bar{u} + u_d) + \bar{y}_e\bar{v}}{\sqrt{\Delta^2 + \bar{y}_e^2}} \\ &\quad + \frac{1 - \cos(z_1)}{z_1} \frac{u_d\bar{y}_e - \Delta\bar{v}}{\sqrt{\Delta^2 + \bar{y}_e^2}} \quad (46)\end{aligned}$$

$$h_{13} = -\cos(z_1) \frac{\bar{y}_e}{\sqrt{\Delta^2 + \bar{y}_e^2}} \quad (47)$$

$$\begin{aligned}h_{21} &= -\left(\frac{\Delta}{\Delta^2 + \bar{y}_e^2}(\Upsilon u_d + M)h_{11} + \Upsilon\frac{\Delta}{\Delta^2 + \bar{y}_e^2}\bar{u}h_{11}\right) \\ &= \frac{-\Delta}{\Delta^2 + \bar{y}_e^2}((\Upsilon u_d + M)h_{11} + \Upsilon\bar{u}h_{11}) \quad (48)\end{aligned}$$

$$h_{22} = (\Upsilon\bar{u} + \Upsilon u_d + M) \quad (49)$$

$$\begin{aligned}h_{23} &= -\left(\frac{\Delta}{\Delta^2 + \bar{y}_e^2}(\Upsilon u_d + M)h_{13} - \Lambda\bar{v}\right. \\ &\quad - \Upsilon\frac{\Delta}{\left(\sqrt{(\Delta^2 + \bar{y}_e^2)}\right)^3}u_d\bar{y}_e + \Upsilon\frac{\Delta^2}{\left(\sqrt{(\Delta^2 + \bar{y}_e^2)}\right)^3}\bar{v}) \\ &\quad - \Upsilon\frac{\Delta}{\Delta^2 + \bar{y}_e^2}h_{13}\bar{u} \\ &= -\frac{\Delta}{\Delta^2 + \bar{y}_e^2}((\Upsilon u_d + M)h_{13} - \Upsilon\frac{u_d\bar{y}}{\sqrt{(\Delta^2 + \bar{y}_e^2)}} \\ &\quad + \Upsilon\frac{\Delta\bar{v}}{\sqrt{(\Delta^2 + \bar{y}_e^2)}} + \Upsilon h_{13}\bar{u}) + \Lambda\bar{v} \quad (50)\end{aligned}$$

Equation (44) represents the internal dynamics of the system and (45) is the controlled external error dynamics. The system (44)–(45) can be written as:

$$\dot{\mathbf{x}} = \mathbf{f}_1(t, \mathbf{x}) + \mathbf{g}(t, \mathbf{x}, \boldsymbol{\xi})\boldsymbol{\xi} \quad (51)$$

$$\dot{\boldsymbol{\xi}} = \mathbf{f}_2(t, \boldsymbol{\xi}) \quad (52)$$

where  $\mathbf{x} = [\bar{y}_e, \bar{v}]^\top$  and  $\boldsymbol{\xi} = [z_1, z_2, \bar{u}]^\top$ .

**Assumption 1** Assume that  $u_d > 0$  is constant and that the look-ahead distance:

$$0 < \frac{1}{2\sqrt{2}-2} \frac{X}{Y} < \Delta \quad (53)$$

for  $X = \Upsilon u_d + M$  and  $Y = \Lambda u_d + N$ .

**Proposition 1** The origin  $(\bar{y}_e, \bar{v}) = (0, 0)$  of the nominal system  $\dot{\mathbf{x}} = \mathbf{f}_1(t, \mathbf{x})$  is USGES under Assumption 1.

**PROOF.** See Appendix B.

**Theorem 2 (USGES/UGAS cascaded system)**

Under Assumption 1 the ship dynamics (25)–(29) with control laws (37)–(38) renders the origin of the cascade (51)–(52) USGES and UGAS.

**PROOF.** It is shown by Fredriksen and Pettersen (2006) that the interconnection term  $\mathbf{g}(t, \mathbf{x}, \boldsymbol{\xi})$  in (51) has linear growth in  $\mathbf{x}$ . Furthermore, the perturbing system (52) is time-invariant, linear and GES. The closed-loop system (51)–(52) thus satisfies the conditions of Loria and Panteley (2004, Proposition 2.3), which guarantees that the origin is USGES and UGAS.

**Remark 4** Note that Loria and Panteley (2004, Proposition 2.3) only requires the perturbing system to be USGES. We used a feedback linearizing control law (37)–(38) that gave GES external error dynamics, but from the proof of Theorem 2 we see that any control law for  $\tau_u$  and  $\delta$  which gives USGES of the external error dynamics provides the same stability result.

**Remark 5** Note that due to the sinusoidal function that saturates the right-hand side of (34), the gain of the cross-track error dynamics (44) is decreasing with increasing  $\bar{y}_e$ . Therefore, global exponential convergence with uniform convergence rate is not possible to achieve.

## 4 Conclusions

In this paper we have presented a uniform semiglobal exponential stability proof for a class of proportional line-of-sight guidance laws used by ancient navigators for vehicle path-following control. This extends previous results that only guarantee global  $\kappa$ -exponential stability. The stability proof can also be used in cascaded stability analysis to ensure uniform semiglobal exponential stability of the total system. Typical applications are marine craft, AUV and UAV motion control systems for path following.

## Acknowledgements

This work was supported by the Norwegian Research Council (project no. 223254) through the Center of Autonomous Marine Operations and Systems (AMOS) at the Norwegian University of Science and Technology.

## A Proof of Theorem 1

The system (17) is nonautonomous since  $U$  and  $\Delta$  are time varying. Consider the Lyapunov function candidate:  $V(t, y_e) = (1/2)y_e^2 > 0$  when  $y_e \neq 0$ . Hence,

$$\dot{V}(t, y_e) = -\frac{U}{\sqrt{\Delta^2 + y_e^2}} y_e^2 \leq 0 \quad (\text{A.1})$$

Since  $V(t, y_e) > 0$  and  $\dot{V}(t, y_e) \leq 0$  it follows that:

$$|y_e(t)| \leq |y_e(t_0)|, \quad \forall t \geq t_0 \quad (\text{A.2})$$

and by Khalil (2002, Theorem 4.8) the origin  $y_e = 0$  is uniformly stable. Next, we define:

$$\phi(t, y_e) := \frac{U}{\sqrt{\Delta^2 + y_e^2}} \quad (\text{A.3})$$

For each  $r > 0$  and all  $|y_e(t)| \leq r$ , we have

$$\phi(t, y_e) \geq \frac{U_{\min}}{\sqrt{\Delta_{\max}^2 + r^2}} := c(r) \quad (\text{A.4})$$

Consequently,

$$\begin{aligned} \dot{V}(t, y_e) &= -2\phi(t, y_e)V(t, y_e) \\ &\leq -2c(r)V(t, y_e), \quad \forall |y_e(t)| \leq r \end{aligned} \quad (\text{A.5})$$

In view of (A.2), the above holds for all trajectories generated by the initial conditions  $y_e(t_0)$ . Consequently, we can invoke the comparison lemma (Khalil, 2002, Lemma 3.4) by noticing that the linear system  $\dot{z} = -2c(r)z$  has the solution  $z(t) = e^{-2c(r)(t-t_0)}z(t_0)$ , which implies that  $\dot{v}(t) \leq e^{-2c(r)(t-t_0)}v(t_0)$  for  $v(t) = V(t, y_e(t))$ . Therefore,

$$y_e(t) \leq e^{-c(r)(t-t_0)}y_e(t_0) \quad (\text{A.6})$$

for all  $t \geq t_0$ ,  $|y_e(t_0)| \leq r$  and any  $r > 0$ . Hence, we can conclude that the equilibrium point  $y_e = 0$  is USGES (Loria and Panteley, 2004, Definition 2.7).

## B Proof of Proposition 1

Let  $\gamma = -2X(1 - \alpha)/(\alpha^3 Y^2 u_d) > 0$ ,  $0 < \alpha < 1$  and

$$\begin{aligned} W(t, \bar{y}_e, \bar{v}) &= (1/2)\bar{y}_e^2 + (\gamma/2)\bar{v}^2 \\ &:= \frac{1}{2} \mathbf{x}^\top \mathbf{P} \mathbf{x} \end{aligned} \quad (\text{B.1})$$

where  $\mathbf{x} = [\bar{y}_e, \bar{v}]^\top$  and  $\mathbf{P} = \text{diag}\{1, \gamma\} > 0$ . Time differentiation of  $W(t, \bar{y}_e, \bar{v})$  gives:

$$\begin{aligned} \dot{W} &= \bar{y}_e \dot{\bar{y}}_e + \gamma \bar{v} \dot{\bar{v}} \\ &= \bar{y}_e \left( \frac{-u_d}{\sqrt{\Delta^2 + \bar{y}_e^2}} \bar{y}_e + \frac{\Delta}{\sqrt{\Delta^2 + \bar{y}_e^2}} \bar{v} \right) \\ &\quad + \gamma \bar{v} \left( X \frac{\Delta u_d}{(\sqrt{(\Delta^2 + \bar{y}_e^2)})^3} \bar{y}_e \right. \\ &\quad \left. + \left( Y - X \frac{\Delta^2}{(\sqrt{(\Delta^2 + \bar{y}_e^2)})^3} \right) \bar{v} \right) \\ &= \frac{-\alpha Y \Delta u_d}{X \sqrt{(\bar{y}_e^2 + \Delta^2)}} \left( \bar{y}_e - \frac{1}{2} \left( \frac{X}{\alpha Y u_d} + \frac{\gamma \alpha Y \Delta^2}{(\bar{y}_e^2 + \Delta^2)} \right) \bar{v} \right)^2 \\ &\quad - \left( -\gamma Y + \frac{1}{2} \frac{\gamma \alpha Y \Delta^3}{(\bar{y}_e^2 + \Delta^2)^{\frac{3}{2}}} - \frac{1}{4\alpha Y} \frac{\Delta}{u_d} \frac{X}{\sqrt{(\bar{y}_e^2 + \Delta^2)}} \right. \\ &\quad \left. - \frac{1}{4} \alpha^3 Y^3 \Delta^5 \frac{u_d}{X (\sqrt{(\bar{y}_e^2 + \Delta^2)})^5} \gamma^2 \right) \bar{v}^2 \end{aligned} \quad (\text{B.2})$$

where  $\alpha = X/\Delta Y$ . Since  $X < 0$ ,  $Y < 0$  and  $0 \leq \Delta/\sqrt{\bar{y}_e^2 + \Delta^2} \leq 1$  for all  $\bar{y}_e$ ,  $\dot{W}$  satisfies:

$$\begin{aligned} \dot{W} &\leq \frac{-\alpha Y \Delta u_d}{X \sqrt{(\bar{y}_e^2 + \Delta^2)}} \left( \bar{y}_e - \frac{1}{2} \left( \frac{X}{\alpha Y u_d} + \frac{\gamma \alpha Y \Delta^2}{(\bar{y}_e^2 + \Delta^2)} \right) \bar{v} \right)^2 \\ &\quad - \left( -\gamma Y + \frac{1}{2} \gamma \alpha Y - \frac{1}{4\alpha Y} \frac{X}{u_d} - \frac{1}{4} \alpha^3 Y^3 \frac{u_d}{X} \gamma^2 \right) \bar{v}^2 \\ &:= -\bar{\phi} \mathbf{x}^\top \mathbf{Q} \mathbf{x} \end{aligned} \quad (\text{B.3})$$

where

$$\bar{\phi}(t, \mathbf{x}) := \frac{u_d}{\sqrt{\bar{y}_e^2 + \Delta^2}} \quad (\text{B.4})$$

$$\mathbf{Q} := \begin{bmatrix} 1 & -\frac{1}{2}\sigma \\ -\frac{1}{2}\sigma & \Pi + \frac{1}{4}\sigma^2 \end{bmatrix} \quad (\text{B.5})$$

and

$$\Pi := \frac{\sqrt{\bar{y}_e^2 + \Delta^2}}{u_d} \left( -\gamma Y + \frac{1}{2}\gamma\alpha Y - \frac{1}{4\alpha Y} \frac{X}{u_d} - \frac{1}{4}\alpha^3 Y^3 \frac{u_d}{X} \gamma^2 \right) \quad (\text{B.6})$$

$$\sigma := \frac{X}{\alpha Y u_d} + \frac{\gamma\alpha Y \Delta^2}{\bar{y}_e^2 + \Delta^2} \quad (\text{B.7})$$

By *Sylvester's theorem*, we see that the matrix  $\mathbf{Q}$  is positive definite if and only if  $\Pi > 0$ . The sign of the bracket term in (B.6) can be determined by substituting  $\gamma = -2X(1 - \alpha)/(\alpha^3 Y^2 u_d) > 0$  into the formula for  $\Pi$ . Then it is easy to verify that  $\Pi > 0$  if and only if  $1 - \alpha - (1/4)\alpha^2 > 0$ . Since  $\alpha$  is required to be positive, this is equivalent to  $0 < \alpha < 2\sqrt{2} - 2$ . Finally,  $\alpha = X/\Delta Y$  verifies that this is satisfied if and only if  $\Delta$  satisfies the upper bound given by Assumption 1.

Recall from (B.3) that  $\dot{W} \leq -\bar{\phi} \mathbf{x}^\top \mathbf{Q} \mathbf{x}$ . Assumption 1 guarantees that  $\mathbf{Q} > 0$ . Since  $W > 0$  and  $\dot{W} \leq 0$  it follows that:

$$\|\mathbf{x}(t)\| \leq \|\mathbf{x}(t_0)\|, \quad \forall t \geq t_0 \quad (\text{B.8})$$

and by Khalil (2002, Theorem 4.8) the origin  $\mathbf{x} = \mathbf{0}$  is uniformly stable. Furthermore, for each  $\bar{r} > 0$  and all  $\|\mathbf{x}(t)\| \leq \bar{r}$ , we have

$$\bar{\phi}(t, \mathbf{x}) \geq \frac{u_d}{\sqrt{\Delta_{\max}^2 + \bar{r}^2}} := c(\bar{r}) \quad (\text{B.9})$$

for any constant surge velocity  $u_d > 0$ . Consequently,

$$\dot{W} \leq -2\bar{\phi} \frac{q_{\min}}{p_{\max}} W \leq -2 \frac{q_{\min}}{p_{\max}} c(\bar{r}) W, \quad \forall \|\mathbf{x}(t)\| \leq \bar{r} \quad (\text{B.10})$$

where  $p_{\max} = \max\{1, \gamma\}$  and  $q_{\min} = \lambda_{\min}(\mathbf{Q})$ . In view of (B.8), the above holds for all trajectories generated by the initial conditions  $\mathbf{x}(t_0)$ . Consequently, we can invoke the comparison lemma (Khalil, 2002, Lemma 3.4) by noticing that the linear system  $\dot{\bar{z}} = -2(q_{\min}/p_{\max})c(\bar{r})\bar{z}$  has the solution  $\bar{z}(t) = e^{-2(q_{\min}/p_{\max})c(\bar{r})(t-t_0)}\bar{z}(t_0)$ , which implies that  $\dot{w}(t) \leq e^{-2(q_{\min}/p_{\max})c(\bar{r})(t-t_0)}w(t_0)$  for  $w(t) = W(t, \mathbf{x}(t))$ . Hence, defining  $p_{\min} = \min\{1, \gamma\}$ :

$$\|\mathbf{x}(t)\| \leq \sqrt{\frac{p_{\max}}{p_{\min}}} e^{-\frac{q_{\min}}{p_{\max}} c(\bar{r})(t-t_0)} \|\mathbf{x}(t_0)\| \quad (\text{B.11})$$

for all  $t \geq t_0$ ,  $\|\mathbf{x}(t)\| \leq \bar{r}$  and any  $\bar{r} > 0$ . Hence, we can conclude that the equilibrium point  $\mathbf{x} = \mathbf{0}$  is USGES (Loria and Panteley, 2004, Definition 2.7).

## References

- M. Breivik and T. I. Fossen (2005). Principles of guidance-based path following in 2D and 3D. In: *Proc. of the IEEE Conf. on Decision and Control, and the European Control Conf.*, Seville, Spain, pp. 627-634.
- M. Breivik and T. I. Fossen (2009). *Guidance laws for autonomous underwater vehicles*. In: *Intelligent Underwater Vehicles*. I-Tech Education and Publishing (A. V. Inzartsev, Ed.), Ch. 4, pp. 51-76, Vienna.
- E. Borhaug and K. Y. Pettersen (2005). Cross-track control for underactuated autonomous vehicles. In: *Proc. of the IEEE CDC'12*, Seville, Spain, pp. 602-608.
- T. I. Fossen (2011). *Handbook of Marine Craft Hydrodynamics and Motion Control*. Wiley.
- E. Fredriksen and K. Y. Pettersen (2006). Global  $\kappa$ -exponential waypoint maneuvering of ships: theory and experiments, *Automatica*, AUT-42(4):677-687.
- A. J. Healey and D. Lienard (1993). Multivariable sliding mode control for autonomous diving and steering of unmanned underwater vehicles. *IEEE Journal of Oceanic Engineering*, JOE-18(3):327-339.
- H. K. Isidori (1989). *Nonlinear Control Systems*. Springer.
- H. K. Khalil (2002). *Nonlinear Systems*. Prentice-Hall.
- A. M. Lekkas and T. I. Fossen (2012). A. M. Lekkas and T. I. Fossen. A time-Varying lookahead distance guidance law for path following. In: *Proc. of the IFAC MCMC'12*, 19-21 September, Arenzano, Italy 2012.
- A. M. Lekkas and T. I. Fossen (2013). Line-of-sight guidance for path following of marine vehicles. Chapter 5, In: *Advanced in Marine Robotics*, LAP LAMBERT Academic Publishing (O. Gal, Ed.), pp. 63-92, 2013.
- A. Loria and E. Panteley (2004). Cascaded nonlinear time-varying systems: analysis and design. Ch. 2. In: *Advanced Topics in Control Systems Theory*, Springer-Verlag London (F. Lamnabhi-Lagarrigue, A. Loria and E. Panteley Eds.), pp. 23-64, 2004.
- A. Pavlov, H. Nordahl and M. Breivik (2009). MPC-based optimal path following for underactuated vessels. In: *Proc. of the IFAC MCMC'12*. Sao Paulo, Brazil, pp. 340-345.
- K. Y. Pettersen and E. Lefeber (2001). Waypoint tracking control of ships. In: *Proc. of the IEEE Conf. on Decision and Control*, Orlando, Florida, pp. 940-945.
- C. Samson (1992). Path following and time-varying feedback stabilization of a wheeled mobile robot. In: *Proc. Int. Conf. ICARCV'92*.
- O. J. Sordalen and O. Egeland (1995). Exponential stabilization of nonholonomic chained systems. *IEEE Trans. on Automatic Control*, TAC-40(1):35-49.
- C. Y. Tzeng (1998). Analysis of the pivot point for a turning ship. *J. of Marine Sci. and Techn.* 6(1):39-44.
- R. Yanushevsky (2011). *Guidance of Unmanned Aerial Vehicles*. CRC Press.